Nonideal Mixing and Phase Separation in Phosphatidylcholine-Phosphatidic Acid Mixtures as a Function of Acyl Chain Length and pH

Patrick Garidel, Christof Johann, and Alfred Blume*

*Fachbereich Chemie, Universität Kaiserslautern, D-67653 Kaiserslautern, Germany

ABSTRACT   The miscibilities of phosphatidic acids (PAs) and phosphatidylcholines (PCs) with different chain lengths (n = 14, 16) at pH 4, pH 7, and pH 12 were examined by differential scanning calorimetry. Simulation of heat capacity curves was performed using a new approach that incorporates changes of cooperativity of the transition in addition to nonideal mixing in the gel and the liquid-crystalline phase as a function of composition. From the simulations of the heat capacity curves, first estimates for the nonideality parameters for nonideal mixing as a function of composition were obtained, and phase diagrams were constructed using temperatures for onset and end of melting, which were corrected for the broadening effect caused by a decrease in cooperativity. In all cases the composition dependence of the nonideality parameters indicated nonsymmetrical mixing behavior. The phase diagrams were therefore further refined by simulations of the coexistence curves using a four-parameter approximation to account for nonideal and nonsymmetrical mixing in the gel and the liquid-crystalline phase. The mixing behavior was studied at three different pH values to investigate how changes in headgroup charge of the PA influences the miscibility. The experiments showed that at pH 7, where the PA component is negatively charged, the nonideality parameters are in most cases negative, indicating that electrostatic effects favor a mixing of the two components. Partial protonation of the PA component at pH 4 leads to strong changes in miscibility; the nonideality parameters for the liquid-crystalline phase are now in most cases positive, indicating clustering of like molecules. The phase diagram for 1,2-dimyristoyl-sn-glycero-3-phosphatidic acid:1,2-dipalmitoyl-sn-glycero-3-phosphorylcholine mixtures at pH 4 indicates that a fluid-fluid immiscibility is likely. The results show that a decrease in ionization of PAs can induce large changes in mixing behavior. This occurs because of a reduction in electrostatic repulsion between PA headgroups and a concomitant increase in attractive hydrogen bonding interactions.

INTRODUCTION

The lipid composition of natural membranes is often very complex and provides different functions for the cells. The formation of domains (microdomains) in the liquid-crystalline phase (which can be caused by a low miscibility of the two components) is an interesting phenomenon that has recently received much attention (Glaser, 1993; Almeida et al., 1993; Vaz, 1994, 1995; Almeida and Vaz, 1995). Domain formation influences several properties of biological membranes, such as water permeability (Carruthers and Melchior, 1983), membrane potential (McLaughlin and Brown, 1981), rate of fusion between adjacent lipid bilayers (Hoekstra, 1982a,b), protein lateral diffusion, and the reactivity of intrinsic proteins imbedded in the bilayer (Verkleij, 1984; Benga and Holmes, 1984; Metcalf et al., 1986; Vaz, 1994). A large number of studies have shown that membrane proteins have certain environmental requirements for optimum activity, some requiring a fluid environment, whereas other need much more rigid surroundings (Lee, 1975a,b; Cronam and Gelman, 1975; Stier and Sackmann, 1973; Berclaz and McConnell, 1981; Berclaz and Geoffroy, 1984; Benga and Holmes, 1984; Tocanne et al., 1994).

Domain formation in the liquid-crystalline phase can provide different proteins with their specific environment for optimal activity (Glaser, 1993; Vaz, 1994, 1995).

The aim of this study is the understanding of pseudobinary lipid mixtures in excess water composed of the zwitterionic phospholipid phosphatidylcholine and the negatively charged (at neutral pH) phospholipid phosphatidic acid. The chain lengths of the two components as well as the pH were varied, and the miscibility behavior was analyzed by differential scanning calorimetry (DSC). The obtained heat capacity curves (cp curves) were fitted with a new simulation model that yields nonideality parameters as a function of composition, temperatures for the coexistence lines, and cooperative unit sizes as a function of composition. From these data we then constructed phase diagrams in a first approximation. These phase diagrams were further refined by simulating them with a model using nonideal, nonsymmetrical mixing behavior in both phases.

Using the phospholipids DMPA, DPPA, DMPC, and DPPC we investigated the following systems:

1. DPPA:DPPC and DMPA:DMPC (both components have the same chain lengths)
2. DPPA:DMPC and DMPA:DPPC (the components have different chain lengths)

The net charge of the phosphatidic acid depends on the pH. Therefore, as an additional variable parameter we changed the pH of the dispersions. DSC measurements of the mixtures were performed at pH 4, pH 7, and pH 12 to study the mixing properties as a function of charge of the

phosphatidic acid component. We will show that the charge and the resulting variations in headgroup interactions as well as the chain length differences will have a marked effect on the miscibilities of the two components in both phases.

MATERIALS AND METHODS

1,2-Dipalmitoyl-*sn*-glycero-3-phosphorylcholine (DPPC), 1,2-dimyristoyl-*sn*-glycero-3-phosphorylcholine (DMPC), 1,2-dipalmitoyl-*sn*-glycero-3-phosphatidic acid (DPPA), and 1,2-dimyristoyl-*sn*-glycero-3-phosphatidic acid (DMPA) were obtained from Natterman Phospholipid GmbH (Cologne, Germany). The purity of the lipids was checked by thin-layer chromatography (TLC), using a phosphorous sensitive spray and charring with concentrated sulfuric acid (Hahn and Luckhaus, 1956). Only one spot was detected on the TLC plate; therefore the lipids were used without further purification.

Lipid stock solutions in $CHCl_3$:CH_3OH (2:1, v:v) were prepared and mixed to obtain homogeneous mixtures at different molar ratios. The solvent was rapidly removed under an argon stream by carefully heating the probes. The dried mixtures were then held for 24 h in high vacuum to remove residual traces of solvent. After drying, the appropriate amount of highly purified water was added, and the samples were vigorously vortexed for 5 min at 75–80°C and additionally for 5 min at room temperature to get a homogeneous dispersion. The pH of the samples was checked and corrected with an appropriate amount of HCl or NaOH. The measurements were done at pH 4, pH 7, and pH 12. The total lipid concentration was 2.5 mg/ml. The pH was measured before and after the DSC experiment. No changes in pH were observed.

DSC measurements were performed with a MicroCal MC-2 differential scanning calorimeter (MicroCal, Northhampton, MA). The heating rate was 1°C/min, and the measurements were performed in the temperature interval from 8°C to 85°C. For a check of the reproducibility of the DSC curves, three scans were usually recorded for studies at pH 4 and pH 7. After the measurements the samples were checked by TLC, and no degradation of the lipids was detected. At pH 12 only the first scan was used for evaluation because of some hydrolysis of the lipids at high pH as detected by TLC after the second run.

Three different samples were measured for each composition to check for reproducible results. The accuracy of the DSC experiments was ±0.1°C for the main phase transition temperature T_m and ±0.2 kcal/mol for the main transition enthalpy ΔH_m.

THEORY AND SIMULATION METHODS

Binary phase diagrams can be easily constructed from DSC thermograms. Usually this is done by the following procedure. The onset and completion temperatures for the gel-to-liquid-crystalline transition are determined as those temperatures corresponding to the intersection between the tangent of the leading edge and the baseline of the DSC curves (Xu et al., 1987; Ali et al., 1989). These temperatures are then corrected by the finite widths of the transitions of the pure components weighted with their mole fractions according to a method described by several authors (Mabrey and Sturtevant, 1976; Silvius and Gagné, 1984a,b).

The determination of these two temperatures is a critical point for the correct construction of a phase diagram. We have developed a different method for the determination of these temperatures by simulation of the heat capacity curves (cp curves) (Mennicke, 1995; Johann et al., 1996), using regular solution theory and incorporating an additional pa-

rameter describing the broadening of the transition due to limited cooperativity. This leads in some cases to phase diagrams with a narrower two-phase region and to additional information on the cooperative unit (c.u.) size as a function of composition. In the following we will give only a brief outline of underlying calculation procedures.

Calculation of the heat capacity curves

We consider a hypothetical phase transition for the lipids with infinitely high cooperativity (Sugár, 1987). We will first derive an expression for the heat capacity curve of a binary mixture of lipids that we will call cp^{id}.

For our binary system with components A and B, the molar enthalpy H as a function of temperature in the phase transition region from the gel to the liquid-crystalline phase can be described by

$$H = \varphi \cdot H_g + (1 - \varphi) \cdot H_1, \tag{1}$$

where H_g and H_1 are the enthalpies in the gel and liquid-crystalline phase, respectively, and φ is the degree of transition going from 1 to 0 in the liquid-crystalline phase. φ can be calculated from the lever rule:

$$\varphi = \frac{x - x_1}{x_g - x_l}, \tag{2}$$

where x_g and x_1 are the mole fractions of component B in the solid and liquid-crystalline phases in equilibrium at a given temperature.

If we assume nonideal mixing in the two phases, we can formulate two equations for the enthalpies H_g and H_1 as a function of composition, introducing an excess enthalpy ΔH^E:

$$H_g = x_A \cdot H_{g,A} + x_B \cdot H_{g,B} + \Delta H_g^E;$$
$$H_1 = x_A \cdot H_{1,A} + x_B \cdot H_{1,B} + \Delta H_1^E. \tag{3}$$

Using the Gibbs-Helmholtz equation $\Delta G^E = \Delta H^E - T \cdot \Delta S^E$, two borderline cases can be postulated, namely the case with $\Delta S^E = 0$, which gives $\Delta G^E = \Delta H^E$ (regular solution) (Hildebrandt, 1929) and the case with $\Delta H^E = 0$ (athermal solution) (Guggenheim, 1944).

For the simulation of the cp curves we will use only regular solution theory. The nonideality of the system is caused by a nonzero ΔH^E.

The free excess enthalpy ΔG^E of mixing as a function of mole fraction x can be written as

$$\Delta G^E = \Delta H^E = x \cdot (1 - x) \cdot \{\varrho_1 + \varrho_2 \cdot (2x - 1) + \varrho_3 \tag{4}$$
$$\cdot (2x - 1)^2 + \varrho_4 \cdot (2x - 1)^3 + \ldots\}.$$

ϱ_i are the nonideality parameters describing the deviations from ideal mixing behavior.

For the simulation of the cp curves we have used a symmetrical formulation for the excess enthalpy for both

phases:

$$\Delta G^E = \Delta H^E = x \cdot (1 - x) \cdot \varrho. \qquad (5)$$

The solidus and liquidus curves are calculated from the two transcendental Eqs. 6 and 7, where $x_A = (1 - x)$, $x_B = x$, ΔH_A, and ΔH_B are the calorimetrically measured main transition enthalpies, and T_A and T_B are the main transition temperatures of the pure components A and B (Tenchov, 1985; Brumbaugh and Huang, 1992; Johann et al., 1996):

$$T = \frac{\Delta H_B + \varrho_1 \cdot (1 - x_1)^2 - \varrho_g \cdot (1 - x_g)^2}{(\Delta H_B/T_B) - R \cdot \ln\{x_1/x_g\}} \qquad (6)$$

$$T = \frac{\Delta H_A + \varrho_1 \cdot (x_1)^2 - \varrho_g \cdot (x_g)^2}{(\Delta H_A/T_A) - R \cdot \ln\{(1 - x_1)/(1 - x_g)\}}. \qquad (7)$$

With the definition of $cp^{id} = (\partial H/\partial T)_p$, the heat capacity curves can be calculated from Eqs. 1, 3, and 5 once the segments of the liquidus and solidus curves of the phase diagram are known. The exact expressions have been described elsewhere (Johann et al., 1996).

The calculated cp^{id} curves assume infinite cooperativity for the transition. In reality, the transition curves for pure lipids are broadened because of limited cooperativity. The cooperativity of the transition will be further lowered by mixing two different lipids together (Sugár, 1987).

The simplest method of including the broadening effect is to assume an equilibrium for a two-state transition between the solid and liquid states:

$$G \rightleftharpoons L, \qquad (8)$$

where G and L denote the two different physical states of the system. The equilibrium constant for such a process is then defined as

$$K = \frac{[L]}{[G]} = \frac{1 - \Theta}{\Theta}. \qquad (9)$$

The brackets represent the amount of lipids in one of the states, and θ is the degree of transition running from 1 (all lipids in the gel state) to 0. With the van't Hoff equation,

$$\left(\frac{\partial \ln K}{\partial T}\right)_p = \frac{\Delta H_{vH}}{R \cdot T^2}, \qquad (10)$$

we can calculate an expression for $(\partial\Theta/\partial T)$ describing the width of the transition as a function of the van't Hoff transition enthalpy ΔH_{vH} (Blume, 1988, 1991; Johann et al., 1996). We now convolute the cp^{id} curve with the broadening function $(\partial\Theta/\partial T)$ to obtain a corrected heat capacity curve cp^{sim}

$$cp^{sim} = cp^{id} \otimes \left(\frac{\partial\Theta}{\partial T}\right). \qquad (11)$$

The procedures described above are implemented in a fit program using the SIMPLEX algorithm to find the best parameter set. As input, the program needs the main transition temperatures, the calorimetrically determined transi-

tion enthalpies ΔH_c of the pure components, and the composition of the mixtures.

The output is the desired simulated cp curve, the nonideality parameters ϱ_g and ϱ_1, and the values of the temperatures that describe the beginning (T_-) and the end (T_+) of the transition, i.e., temperatures on the liquidus and solidus curves calculated for a binary mixture where the components show a true first-order phase transition. It turns out that in many cases the nonideality parameters are a function of composition, indicating nonideal, nonsymmetrical mixing behavior. Therefore, in a second step, the T_- and T_+ values are used for the simulation of the phase diagram using an approach for a nonsymmetrical regular solution, which will be described below. A further piece of information obtained by the simulation of the cp curves of the mixtures is the van't Hoff enthalpy ΔH_{vH} as a function of composition. It allows the calculation of the cooperative unit size, c.u. $= \Delta H_{vH}/\Delta H_c$, for the different mixtures.

Simulation of phase diagrams

For the simulation of the phase diagrams we use a formulation with four nonideality parameters, taking the nonsymmetrical mixing into account. From Eq. 4 we then obtain for each of the two phases an expression for the excess free energy and enthalpy of mixing:

$$\Delta G^E = \Delta H^E = x \cdot (1 - x) \cdot [\varrho_1 + \varrho_2 \cdot (2 \cdot x - 1)]. \qquad (12)$$

This leads us to a pair of equations of coexistence, which give us the four nonideality parameters: ϱ_{11} and ϱ_{12}, ϱ_{g1} and ϱ_{g2}. The equations for coexistence have the following form:

$$T = \frac{\begin{matrix}\Delta H_B + (1 - x_1)^2 \cdot \{\varrho_{11} + \varrho_{12} \cdot (4x_1 - 1)\} \\ - (1 - x_g)^2 \cdot \{\varrho_{g1} + \varrho_{g2} \cdot (4x_g - 1)\}\end{matrix}}{(\Delta H_B/T_B) - R \cdot \ln\{x_1/x_g\}} \qquad (13)$$

$$T = \frac{\begin{matrix}\Delta H_A + (x_1)^2 \cdot \{\varrho_{11} + \varrho_{12} \cdot (4x_1 - 3)\} \\ - (x_g)^2 \cdot \{\varrho_{g1} + \varrho_{g2} \cdot (4x_g - 3)\}\end{matrix}}{(\Delta H_A/T_A) - R \cdot \ln\{(1 - x_1)/(1 - x_g)\}}. \qquad (14)$$

A more detailed derivation of these equations is given by Johann et al. (1996).

A positive ϱ reflects immiscibility between unlike lipids, resulting in the lateral phase separation and domain formation of lipids of the same type and in the same phase. Negative ϱ values reflect a tendency to ordered, "chessboard"-type mixing of the two lipids in the membrane plane. The problem in the simulation of phase diagrams is the fact that combinations of nonideality parameters for the two phases with the same difference $\Delta\varrho = \varrho_1 - \varrho_g$ have in a certain range of values only a marginal effect on the shape of the phase diagram (Brumbaugh and Huang, 1992). The temperatures of onset and completion of melting therefore have to be known with great precision to obtain reliable absolute values for the nonideality parameters (Johann et al., 1996). More reliable is the difference between the non-

ideality parameters $\Delta\varrho$:

$$\Delta\varrho = \varrho_l - \varrho_g. \qquad (15)$$

We will therefore base our discussion later mainly on these $\Delta\varrho$ values.

Monte Carlo simulation of lipid lateral distribution

Monte Carlo simulations for lateral lipid distributions in the liquid-crystalline phase were carried out on a 80 × 80 two-dimensional triangular lattice with standard periodic boundary conditions using fixed mole fractions x and non-ideality parameters determined from the simulations of the phase diagram and a temperature of 330K. To bring the system into equilibrium, the Kawasaki method was used (Kawasaki, 1972; Jan et al., 1984). For the simulations of distribution at pH 7, the pure phases of the two components were used as a start configuration. The number of Monte Carlo steps used was 6–7 · 10^7. Equilibrium was reached after 6 · 10^7 steps. For simulations at pH 4, a random configuration of the two components was used as the start configuration. In this case it was necessary to use 9 · 10^8 Monte Carlo steps to reach equilibrium.

RESULTS

Pure components

The results for the pH dependence of the main transition of the four phospholipids studied are summarized in Table 1. The results for DMPA and DPPA are in agreement with previous data (Träuble and Eibl, 1974; Verkleij et al., 1974; Eibl and Blume, 1979; Blume and Eibl, 1979; Blume and Tuchtenhagen, 1992). Under conditions of low ionic strength (1–4 mM), PAs are singly charged at pH 7, the apparent pK_2 being ~9, and at pH 4 they are partly protonated, the apparent pK_1 being ~3.8 (Eibl and Blume, 1979). A 10-fold increase in the ionic strength decreases the apparent pK values by ~1 unit (Tokutomi et al., 1980).

For the zwitterionic phosphatidylcholines, a slight decrease in T_m with increasing pH is observed, but this effect is much less than for phosphatidic acids. Lowering the pH also has no great influence on the main transition of the PCs, because the pK of the phosphodiester group is much lower. The pretransition is a little more sensitive to pH changes (see Table 2). The results shown for measurements at high

pH are from the first scan when lipid hydrolysis at pH 12 is still negligible (see Materials and Methods).

Pseudobinary systems

The DSC thermograms obtained from the four binary systems at pH 4, pH 7, and pH 12 are shown in Figs. 1–5. The solid lines are the experimentally measured curves, and the dotted lines are the simulated heat capacity curves cp^{sim}. To check whether prolonged incubation of the lipid samples at low temperature had any effect on the DSC curves, we did a complete analysis of DMPA:DPPC mixtures at pH 4.0 and pH 7.0, where the samples had been incubated at 3°C for at least 6 days. For the pure DPPC the subtransition is clearly evident at both pH values, whereas the DSC curves for the other mixtures show no subtransitions and no significant differences in the shape of the peaks compared to nonincubated samples.

Although the simulations of the DSC curves of the PA/PC mixtures at pH 7 and pH 4 give satisfactory fits to the experimental curves, this is not so for mixtures at pH 12. In this case, the assumed model for the mixing behavior using only two nonideality parameters (see above) seems to be too simple. The cp curves are broad, and very complex structures of the thermograms are often seen, which implies a much more sophisticated phase behavior (see DMPA: DMPC or DMPA:DPPC at pH 12). In general, the DSC curves at pH 12 begin at low temperatures with a relatively sharp peak followed by a gradual decrease in the excess heat capacity, so that the thermogram extends over quite a wide temperature range. This is particularly evident for the system DPPA:DMPC and even more for DMPA:DMPC. A different behavior is observed for the system DMPA:DPPC at pH 12. Here the sharp peak is observed at a higher temperature.

Because the cp curves at pH 4 and pH 7 show better fits using our model, we only constructed phase diagrams from experimental curves recorded at these two pH values. The resulting temperatures T_- and T_+ obtained from the simulations are plotted in Figs. 6–9. Again, for the DMPA: DPPC system, the T_- and T_+ values for the samples incubated for prolonged times at low temperature (Fig. 8, crosses) are almost exactly the same as those for the nonincubated samples.

Based on the T_- and T_+ data from the simulations, the phase diagrams were then calculated using the four-param-

TABLE 1 Thermodynamic data for the main phase transition of the pure phospholipids

Lipid	pH 4.0			pH 7.0			pH 12.0		
	T_m (°C)	$T_{1/2}$ (°C)	ΔH_c (kcal/mol)	T_m (°C)	$T_{1/2}$ (°C)	ΔH_c (kcal/mol)	T_m (°C)	$T_{1/2}$ (°C)	ΔH_c (kcal/mol)
DMPC	24.3	0.7	6.44	24.0	0.5	7.35	23.6	1.3	6.37
DMPA	52.9	1.2	5.89	51.3	1.4	7.18	21.5	2.1	4.02
DPPC	41.5	1.2	8.30	41.6	0.5	8.45	40.8	0.5	8.17
DPPA	65.4	1.5	6.90	64.7	1.1	7.74	42.7	1.1	5.69

T_m, Main phase transition temperature; $T_{1/2}$, half-width of transition; ΔH_c, calorimetrically measured transition enthalpy.

TABLE 2 Thermodynamic data for the pretransition of the pure PCs

Lipid	pH 4.0			pH 7.0			pH 12.0		
	T_p (°C)	$T_{1/2}$ (°C)	ΔH_c (kcal/mol)	T_p (°C)	$T_{1/2}$ (°C)	ΔH_c (kcal/mol)	T_p (°C)	$T_{1/2}$ (°C)	ΔH_c (kcal/mol)
DMPC	14.0	1.5	0.61	15.3	1.5	1.32	—	—	—
DPPC	35.9	2.4	1.13	34.5	2.3	1.61	34.4	3.0	0.83

eter model for nonideal mixing described above. The differences in the nonideality parameters between the liquid-crystalline and gel phases are indicated in Figs. 6–9 as $\Delta\varrho_1 = \varrho_{l1} - \varrho_{g1}$ and $\Delta\varrho_2 = \varrho_{l2} - \varrho_{g2}$, the latter value describing the difference in asymmetry in the miscibility behavior between the liquid-crystalline and the gel phases (see Eq. 12). Because the total $\Delta\varrho$ value is described by $\Delta\varrho = \Delta\varrho_1 + \Delta\varrho_2(2x - 1)$, the second term vanishes at $x = 0.5$, and then $\Delta\varrho = \Delta\varrho_1$.

The phase diagrams were calculated, neglecting the complications arising from the pretransition in pure PCs. As can be seen from the DSC curves in Fig. 1–5, the pretransition is absent in all mixtures with 20 mol% or more of the PA component. Below this PA content we would expect at some temperature a three-phase coexistence between L_α and two different gel phases. Taking this effect into account would require a much more complicated model for the simulations. Because the larger part of the phase diagram is not influenced by this effect, we used this simplified approach of assuming only one gel and one liquid-crystalline

phase. Our main interest was the location and curvature of the upper phase boundary and not the gel state behavior. The shape of the upper phase boundary is mainly determined by the mixing behavior in the liquid-crystalline state. We therefore believe that the simplification we have used does not influence our results on the liquid-crystalline mixing behavior to a large extent.

Fig. 10 shows the $\Delta\varrho$ values obtained from the direct simulation of the heat capacity curves using the two-parameter model described above. In Fig. 11 the size of the cooperative unit (c.u.) as a function of composition obtained from the simulation of the cp curves is shown. The general trend is obvious. The cooperative unit size decreases in the mixtures in correspondence with suggestions based on model calculations (Sugár, 1987). The inclusion of the broadening effect due to limited cooperativity in the determination of the temperatures for onset and end of melting leads to phase diagrams that are, in some cases, much narrower than those determined by the usual procedures (Johann et al., 1996). The nonideality parameters deter-
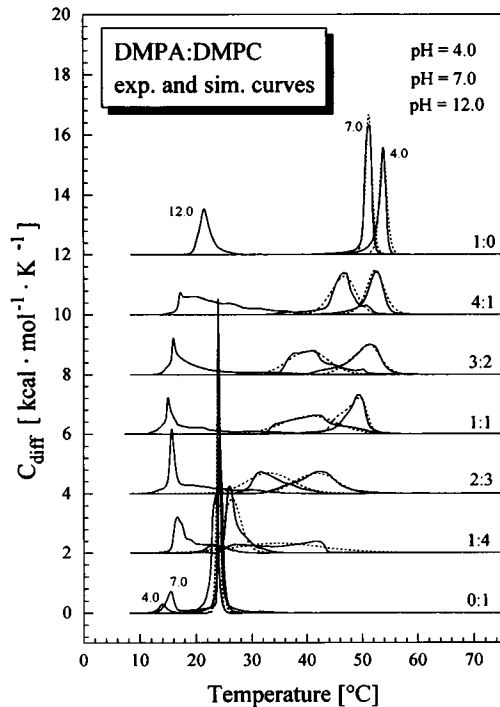

FIGURE 1 DSC heating thermograms for the system DMPA:DMPC at various compositions (molar ratios) at pH 12, pH 7, and pH 4: experimental cp curves (———) and simulated cp curves (– – –).
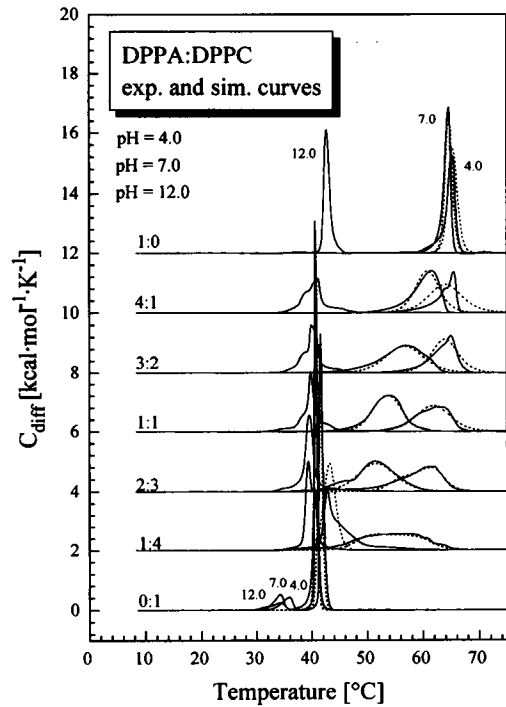

FIGURE 2 DSC heating thermograms for the system DPPA:DPPC at various compositions (molar ratios) at pH 12, pH 7, and pH 4: experimental cp curves (———) and simulated cp curves (– – –).
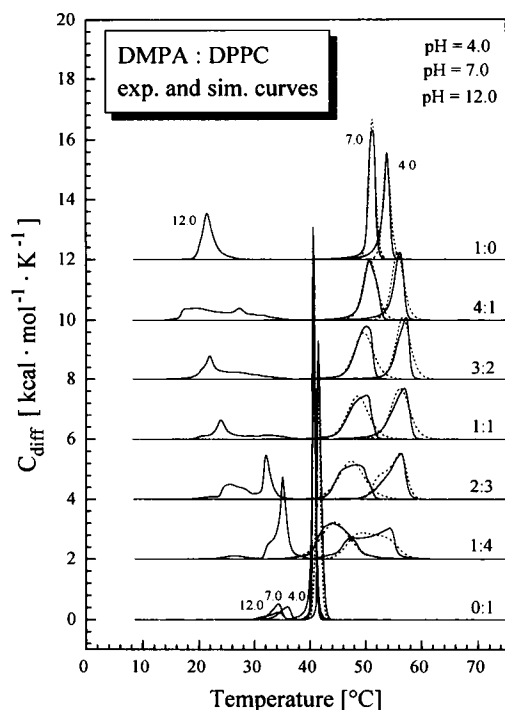
FIGURE 3   DSC heating thermograms for the system DMPA:DPPC at various compositions (molar ratios) at pH 12, pH 7, and pH 4: experimental cp curve (———) and simulated cp curve (- - -).
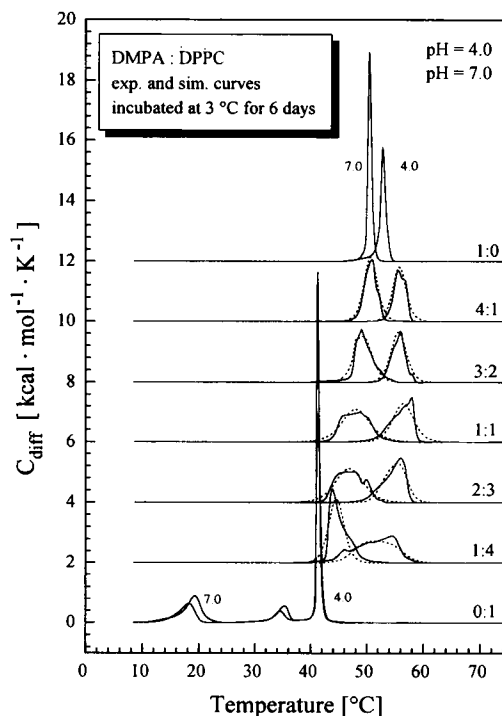

FIGURE 4   DSC heating thermograms for the system DMPA:DPPC at various compositions (molar ratios) at pH 7 and pH 4, incubated for 6 days at 3°C: experimental cp curves (———) and simulated cp curves (- - -).

mined by our procedure are therefore lower than those calculated on the basis of the empirically determined T_- and T_+ values.

DMPA:DMPC

pH 7. The phase diagram for DMPA:DMPC at neutral pH, where DMPA is singly charged, indicates only a small difference in mixing behavior for mixtures in the range x_{DMPA} = 0.4–0.7. However, a considerable change in asymmetry of the miscibility is indicated by the positive $\Delta\varrho_2$ value. The $\Delta\varrho$ values determined by the simulation of the heat capacitiy curves are shown in Fig. 10. They are negative at low concentrations of DMPA but increase with increasing X_{DMPA}. This increase agrees with the positive $\Delta\varrho_2$ value obtained from the simulation of the phase diagram (see Fig. 6). As mentioned above, the absolute values of the nonideality parameters determined from the simulation of the phase diagrams are less reliable than the differences. However, the signs of the ϱ_1 values are definitely negative with approximately -600 to -900 cal/mol. For the gel phase, the mixture seems to be more or less symmetrical, whereas for the liquid-crystalline phase the nonideality increases with decreasing DMPA content.

pH 4. At pH 4 DMPA is partly protonated. The electrostatic effects on the mixing behavior should therefore be reduced. The phase diagram of the system changes, and at low DMPC concentrations in particular, the two-phase region widens considerably compared to the phase diagram at

pH 7. The absolute ϱ_1 values are negative for the gel phase but positive for the liquid-crystalline phase. The $\Delta\varrho$ values for this system are therefore high and positive and the asymmetrical behavior in both phases is similar, so that the $\Delta\varrho$ values are almost independent on composition (see Fig. 10).

DPPA:DPPC

pH 7. The DPPA:DPPC system (Garidel, 1993) should behave in a manner similar to that of the DMPA:DMPC system, because only the chain length of both components has been increased. This is indeed the case, as the thermograms in Fig. 2 and the phase diagrams in Fig. 8 show. It is known that elongating the chains of the phospholipids reduces the headgroup effects, leading to transition temperatures that are closer together. Here we also see this effect in a narrowing of the two-phase region. The ϱ_1 values for both phases are strongly negative, the difference between them being almost zero. The $\Delta\varrho$ values determined from the simulations of the cp curves show a similar trend, and the simulation of the phase diagram using the four-parameter model again leads to an asymmetry in mixing behavior, which is observable as a strongly positive $\Delta\varrho_2$ value.

pH 4. At pH 4, the similarity of the DPPA:DPPC phase diagram to the corresponding C_{14} analogs is also evident, but there are some subtle differences. In this system, the liquidus line reaches a temperature of nearly 63°C at x_{DPPA} = 0.4, and the rest of the coexistence line has then
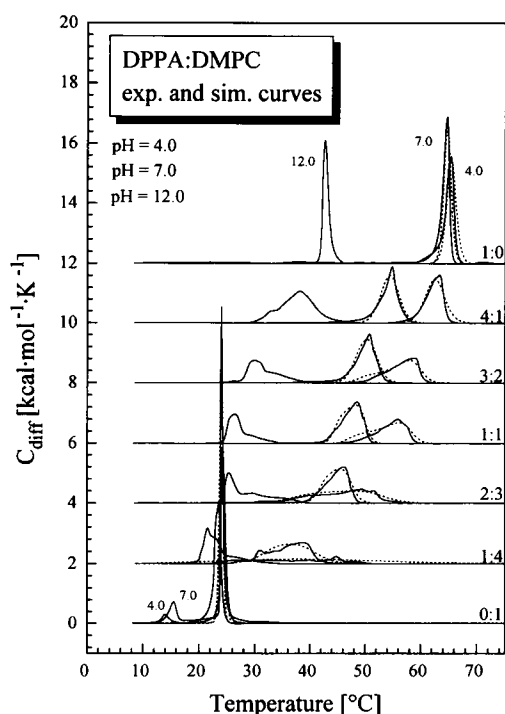
FIGURE 5   DSC heating thermograms for the system DPPA:DMPC at various compositions (molar ratios) at pH 12, pH 7, and pH 4: experimental cp curves (———) and simulated cp curves (- - -).

FIGURE 6   Pseudobinary phase diagrams for the system DMPA:DMPC mixtures at pH 4 and pH 7 constructed from the simulated cp curves. T_- and T_+ were obtained from the simulation of the cp curves ($\triangle$, $\blacktriangledown$). The solid lines are coexistence lines calculated using the four-parameter, nonideal, nonsymmetrical mixing model described in the text. The nonideality parameters were obtained from a nonlinear least-squares fit of the experimental data.

only a small positive slope. At $x_{DPPA} = 0.7$ the solidus line almost touches the liquidus line, and the resulting coexistence range is very narrow. The absolute ϱ_1 values are positive for the liquid-crystalline phase and negative for the gel phase, resulting again in a large positive $\Delta\varrho_1$ value. However, the asymmetry of the mixing behavior is larger than in case of the system DMPA:DMPC.

DMPA:DPPC

pH 7. Reducing the chain length of the phosphatidic acid component leads to phase transition temperatures of the two components, which are very close together. Consequently, we get a phase diagram with a very narrow coexistence range (see Figs. 3, 4, and 8). The mixture shows little nonideal mixing behavior in the liquid-crystalline phase, but in the gel phase the ϱ_1 value is still negative. The asymmetry for the two phases is almost the same, so the $\Delta\varrho$ values are positive at 200 cal/mol and almost constant over the whole composition range. The $\Delta\varrho$ values from the simulations of the heat capacity curves and from the phase diagram agree very well (see Figs. 8 and 10).

pH 4. The ϱ_{11} value for the liquid-crystalline phase is very high and positive for this system, but the asymmetry in the fluid phase is low. For the gel phase the ϱ_{g1} value is also positive, but the asymmetry in mixing is larger, leading to a strong composition dependence for the $\Delta\varrho$ value (see Fig. 10), which is supported by the results obtained from the simulation of the complete phase diagram (see Fig. 8). The
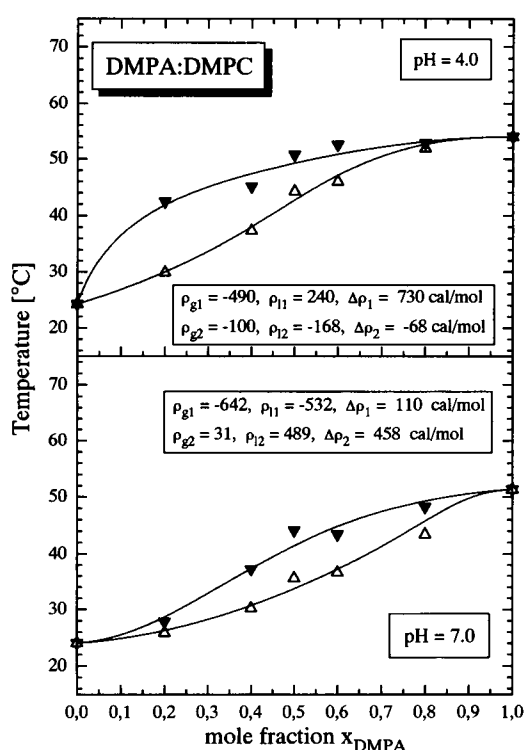
phase diagram indicates that we either have an azeotropic point at $x_{DMPA} = 0.62$ where the liquidus and solidus curves touch, or even an immiscibility region in the liquid-crystalline phase between $x_{DMPA} \approx 0.3$ and $x_{DMPA} \approx 0.7$, because the liquidus line could be horizontal in this composition range. This can also be seen directly from the experimental thermograms in Figs. 3 and 4. The assumption of a miscibility gap in the liquid-crystalline phase means that the formation of fluid lipid domains with different compositions must be considered.

DPPA:DMPC

pH 7. When the chains of the phosphatidic acid component are longer than those of the phosphatidylcholine, the difference between the transition temperatures becomes much larger. For the system DPPA:DMPC this difference is now 40°C. The resulting phase diagram should show a wider two-phase region. This is indeed the case, as seen in Figs. 5 and 9. The phase diagram has a peculiar shape caused by differences in the sign of the ϱ_2 values of the two phases. The ϱ_1 values are again both negative, and the difference $\Delta\varrho$ determined from the simulation of the heat capacity curves is positive but has a pronounced composi-
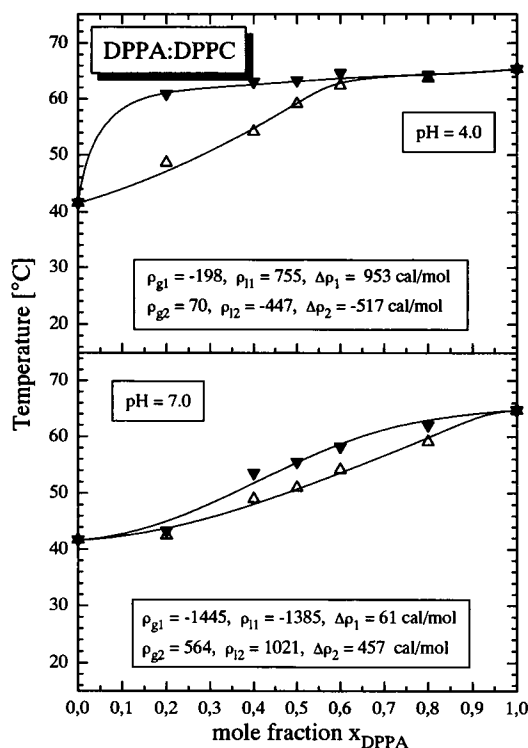
FIGURE 7 Pseudobinary phase diagrams for the system DPPA:DPPC mixtures at pH 4 and pH 7 constructed from the simulated cp curves. T_- and T_+ were obtained from the simulation of the cp curves ($\triangle$, $\blacktriangledown$). The solid lines are coexistence lines calculated using the four-parameter, nonideal, nonsymmetrical mixing model described in the text. The nonideality parameters were obtained from a nonlinear least-squares fit of the experimental data.

FIGURE 8 Pseudobinary phase diagrams for the system DMPA:DPPC mixtures at pH 4 and pH 7 constructed from the simulated cp curves. T_- and T_+ were obtained from the simulation of the cp curves of nonincubated samples ($\triangle$, $\blacktriangledown$) and from samples incubated for 6 days at 3°C (+). The solid lines are coexistence lines calculated using the four-parameter, nonideal, nonsymmetrical mixing model described in the text. The nonideality parameters were obtained from a nonlinear least-squares fit of the experimental data.

tion dependence caused by a strongly negative $\Delta\varrho_2$ value (see Figs. 9 and 10).

pH 4. When DPPA is partly protonated at pH 4, the two-phase region becomes wider. As observed before for the other mixtures, the ϱ_1 values generally increase when the pH is lowered, leading to a shift of the upper phase boundary to higher temperatures. In this case the ϱ_1 value is still negative for the gel phase but already positive for the liquid-crystalline phase. The asymmetry is somewhat lower. In general, the shape of the phase diagram changes in a way similar to that observed for the other mixtures.

PA:PC mixtures at pH 12

As shown in Figs. 1–3 and 5, the DSC peaks shift to lower temperatures when the phosphatidic acid component is in its doubly charged state. We were not able to get satisfactory fits with our program for the simulation of the cp curves. Obviously, the model assumption with two nonideality parameters used in this program is too simple. We have therefore constructed "phase diagrams," using the usual procedure with empirically determined temperatures for the onset and end of melting. The temperatures for onset and end of melting are shown in Fig. 12. They have been
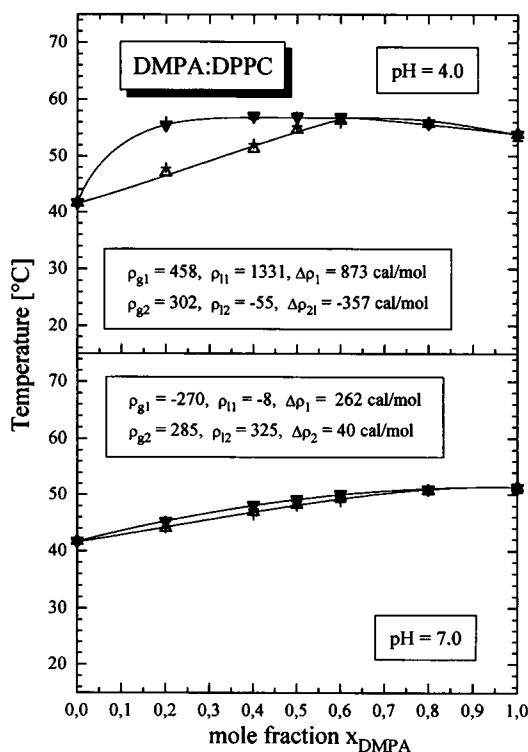
connected by dashed lines just to guide the eye. It is evident that for the systems DMPA:DMPC and DPPA:DPPC the temperatures determined by this procedure do not allow a reliable simulation of the phase diagram, because the curvature of the coexistence lines violates the phase rules. The reason for this is that the transition temperatures of the two components are too close together and the procedure for determining the temperatures of onset and end of melting does not take into account the reduction of the cooperativity of transition in the mixtures, so that the resulting two-phase regions are too wide. This is also true for the DMPA:DPPC system. The general trend is that both phase boundaries are strongly shifted to lower temperatures. Because of these problems we have not simulated these phase diagrams.

DISCUSSION

The heat capacity curves of pseudobinary mixtures of a zwitterionic phospholipid (PC) and a negatively charged phospholipid (PA) as a function of pH were simulated with a model accounting for nonideal mixing in the gel as well as the liquid-crystalline phase, and with an additional parameter describing the broadening of the transition due to limited cooperativity of the transition. These simulations gave
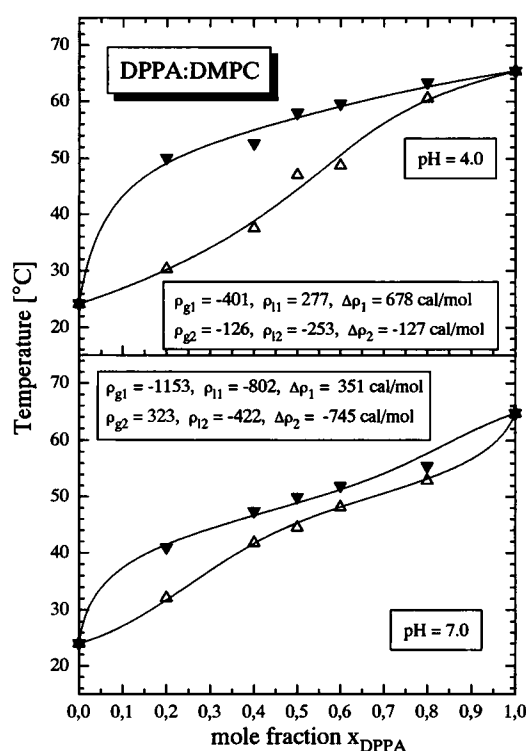
FIGURE 9   Pseudobinary phase diagrams for the system DPPA:DMPC mixtures at pH 4 and pH 7 constructed from the simulated cp curves. T_- and T_+ were obtained from the simulation of the cp curves ($\triangle$, $\blacktriangledown$). The solid lines are coexistence lines calculated using the four-parameter, nonideal, nonsymmetrical mixing model described in the text. The nonideality parameters were obtained from a nonlinear least-squares fit of the experimental data.

FIGURE 10   Difference in nonideality parameters $\Delta\varrho = \varrho_1 - \varrho_g$ for the PA/PC mixtures at pH 4 and pH 7 obtained from the simulation of the cp curves.

satisfactory fits for systems only at pH 4 and 7, whereas the model was apparently too simple for describing the transitions of mixtures at pH 12. From the simulation of the heat capacity curves, temperatures T_- and T_+ for onset and end of melting were obtained. The temperatures obtained in this way indicated narrower two-phase regions than those obtained by the usual empirical procedure where the transitions were only corrected by the width of the transition of the pure components. The results of the simulations were nonideality parameters that depended on composition. In addition, the simulations yielded numbers for the size of the cooperative unit as a function of composition.

The cooperative unit (c.u.) size of the different PA/PC mixtures is shown in Fig. 11. In general, we see that the PCs have higher c.u. values than the corresponding PAs. At pH 7 we find a c.u. for the four lipids: $c.u._{DPPC} = 585$, $c.u._{DMPC} = 127$, $c.u._{DPPA} = 293$, and $c.u._{DMPA} = 76$. At pH 4 all of these values are considerably reduced. If we compare the cooperative unit size of the mixtures with the values of the pure components, we see that the c.u. values in the mixture are considerably lower. The cooperative unit size describes the number of molecules in a domain that changes their physical state abruptly. A sharp phase transition implies a large c.u. value. The U form of the diagrams
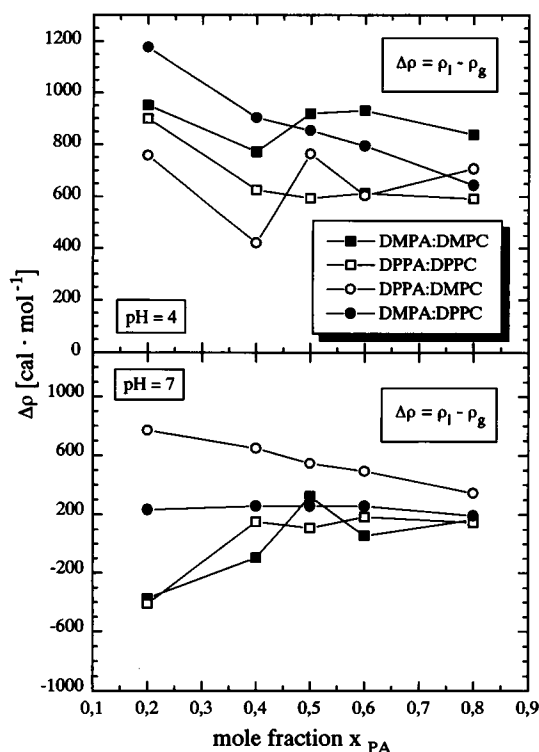
in Fig. 11 is a shape that has been postulated before for pseudobinary lipid systems by Sugár (1987). Here we provide the experimental evidence that this effect occurs. However, we must consider the fact that the simulations of the cp curves were always performed with a constant value for the cooperative unit size. In reality, this changes with temperature, as shown by Sugár (1987). What we present here is only an average value for the whole temperature range of the transition, but it reflects fairly accurately the expected composition dependence.

As mentioned above, the simulation of the heat capacity curves showed that the nonideality parameters were a function of composition. Therefore, the phase diagrams determined from the T_- and T_+ values were now refined and simulated with a thermodynamic model based on the four-parameter approximation for nonideal, nonsymmetrical mixing. This approach gave better fits than the usual two-parameter approach.

Pseudobinary systems at pH 7

As expected, the phase diagrams of binary mixtures where both components have the same chain lengths (DMPA: DMPC and DPPA:DPPC) have very similar shapes. The coexistence region for the DPPA:DPPC system is narrower than for the system DMPA:DMPC because of a decrease in the headgroup influence with increasing chain length. The
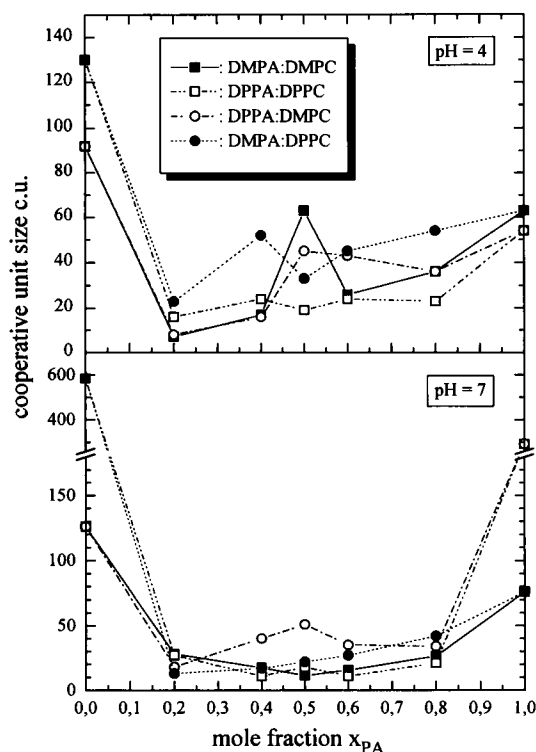
FIGURE 11　Cooperative unit size (c.u.) for the PA/PC systems at pH 4 and pH 7 obtained from the simulations of the cp curves.
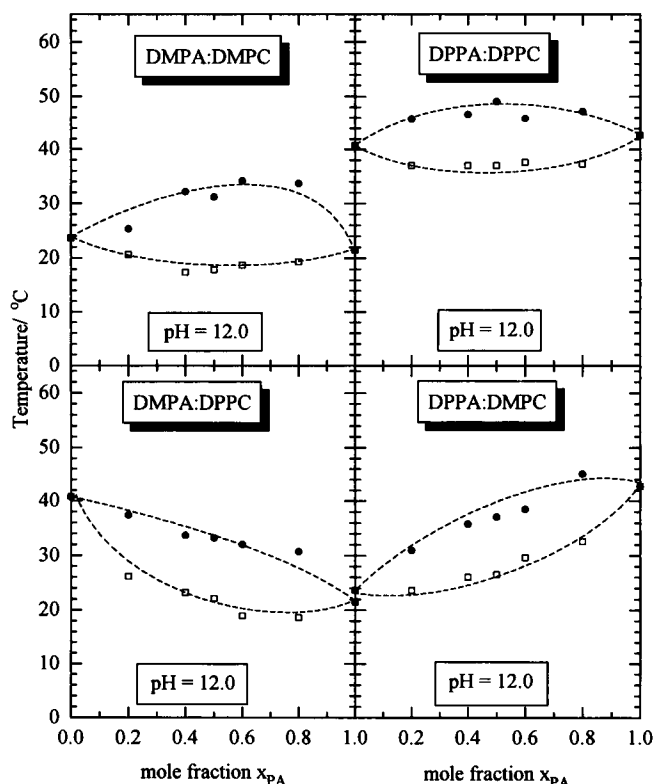

FIGURE 12　Plot of the temperatures for onset and end of melting for the systems DMPA:DMPC, DPPA:DPPC, DPPA:DMPC, and DMPA:DPPC at pH 12 constructed from the experimental cp curves. The values for T_- and T_+ were in this case obtained by the standard empirical procedure and not by simulations of the cp curves. The dashed lines were not simulated, but only drawn to guide the eye. In some cases the curvature of the "coexistence lines" violates the phase rules, showing that the dashed lines have no physical meaning.

difference in the nonideality parameters $\Delta\varrho_1$ and $\Delta\varrho_2$ obtained from the simulations of the phase diagrams have nearly the same values for the two systems. For the C_{14} system we find $\Delta\varrho_1 = 110$ cal/mol and $\Delta\varrho_2 = 458$ cal/mol; the C_{16} system has values of $\Delta\varrho_1 = 61$ cal/mol and $\Delta\varrho_2 = 457$ cal/mol. $\Delta\varrho$ is defined as the difference in the nonideality parameters in the fluid phase and the gel phase. Because of the total difference in the nonideality parameter, $\Delta\varrho = \varrho_1 - \varrho_g = \Delta\varrho_1 + \Delta\varrho_2 \cdot (2x - 1)$, we see that at $x = 0.5$, $\Delta\varrho$ is small but increases with increasing phosphatidic acid content. At low phosphatidic acid content $\Delta\varrho$ is negative. A similar but quantitatively nonidentical result is obtained from the simulation of the cp curves. Here the $\Delta\varrho$ values show considerable scatter (see Fig. 10), but the same trend is obvious, namely positive $\Delta\varrho$ values at high phosphatidic acid content.

A positive $\Delta\varrho$ can be interpreted in different ways. If we assume ideal mixing in the liquid-crystalline phase, it would mean a negative nonideality parameter for the gel phase; this corresponds to complex formation in the ordered phase. If we assume a positive ϱ_g value for the gel phase, indicating immiscibility, it would mean an even more positive ϱ_1 value for the liquid-crystalline phase, i.e., a larger immiscibility. We mentioned above that the reliability of the absolute ϱ values is less than for the differences. However, in both of our simulations all absolute ϱ_1 values are negative for both phases. This means that the nonideality is such that we have a type of complex formation between phosphatidic

acid and phosphatidylcholine in both phases. This tendency for complex formation decreases with increasing PA content in the liquid-crystalline phase more strongly than in the gel phase, because we have positive $\Delta\varrho_2$ values for both the DPPA:DPPC as well as the DMPA:DMPC system.

Usually ϱ_g and ϱ_1 are positive when lipids with identical headgroups but different chain lengths are mixed, ϱ_g having the more positive value, which indicates that miscibility in the gel phase is lower (Nibu et al., 1995). In our case, this is not so, and this is obviously caused by the charge of the headgroup. The additional ΔG^E term due to electrostatic effects has been calculated before on the basis of the Gouy-Chapman theory by Träuble and co-workers (Träuble, 1976; Träuble et al., 1976). As expected, this term is negative, and for a symmetrical mixture it has a maximum at a mole fraction of $x = 0.5$ with a value of -350 cal/mol at 0.1 M ionic strength. The values for $\Delta G^E = \Delta H^E$ we obtain from the simulations of the two phase diagrams are approximately -250 cal/mol. So they are indeed in the correct range. However, to assign the deviations from ideal mixing purely to electrostatic effects is certainly an oversimplification. Additional effects arising from attractive forces via

hydrogen bonds between PA molecules must be taken into account. These are apparently the causes for the lower ΔG^E value and the nonsymmetrical behavior of the mixtures.

When, in addition, a chain length difference between PC and PA is introduced, we can expect a different phase behavior, depending on whether the PC has the shorter chain or vice versa. For DMPA:DPPC mixtures a very narrow coexistence range is observed, because the transition temperatures of the components are close together. Both ρ values are again negative, with $\rho_g < \rho_l$, so that $\Delta\rho > 0$. For both phases the asymmetry is essentially the same and varies in the same direction as observed before. At high PA content, ρ_l becomes positive, whereas ρ_g is close to zero.

In the system DPPA:DMPC, the phase transition temperatures are far apart. Consequently, we would expect an increase in nonideal behavior in the direction of demixing, i.e., positive ρ values, because of the chain length differences. However, the opposite effect is observed: both ρ values are strongly negative with $\rho_l > \rho_g$. This system also shows the highest positive $\Delta\rho$ value of all mixtures at pH 7. The peculiar shape of the phase diagram is a result of different signs of the ρ_2 values for the gel and liquid-crystalline phases. At high PA content the ρ_1 value becomes more negative, whereas the opposite is true for ρ_g. This leads to a decrease in the positive $\Delta\rho$.

Summarizing, we can say that the ρ_1 values for all mixtures are negative, for the gel as well as for the liquid-crystalline phase. This indicates that the nonideal behavior is caused by electrostatic effects—the repulsive interaction between the negatively charged PA molecules leads to "complex formation." An alternative (or, rather, additional) possibility for explaining the negative ρ values is that hydrogen bonds between PC-PA headgroups are stronger than between like PA molecules.

When we compare the $\Delta\rho_1$ values indicative for the differences in mixing behavior between liquid-crystalline and gel phase, we find that they are positive but relatively small and cover a range from 60 to 350 cal/mol, the values being larger for mixtures with unequal chain length. Therefore, electrostatic effects in terms of repulsive interactions and/or the hydrogen bonding effects between unlike headgroups are reduced in the liquid-crystalline phase. The asymmetrical behavior of the mixtures depends on the chain length differences and the differences in chain melting temperature. For DPPA:DMPC, the system with the largest differences in T_m, the asymmetry in mixing behavior has a different sign for the gel phase compared to the liquid-crystalline phase.

Pseudobinary systems at pH 4

Changing the pH to 4 decreases the charge of pure PAs to approximately -0.6 elementary charges (Eibl and Blume, 1979; Blume and Eibl, 1979). Theoretically, we must consider a composition-dependent apparent pK in mixtures of PA with PC, because the apparent pK depends on the

surface charge density (Träuble et al., 1976). We would expect that for low PA content the charge of the phosphatidic acid is higher than for high PA content. Surprisingly, the effects of changing the pH to 4 on the DSC thermograms seems to be more pronounced for lower PA content, in contrast to the expectations. Regardless of the exact degree of protonation of the PA component in these mixtures, the electrostatic effect on the Gibbs free energy of mixing, which is negative, should be reduced. Superimposed on this effect is the increased ability to form hydrogen bonds with neighboring molecules when the PA headgroups are partly protonated. In pure PAs this leads to the maximum in the T_m value as a function of pH (Eibl and Blume, 1979; Blume and Eibl, 1979). This increase in T_m is observed for all mixtures. We therefore believe that additional hydrogen bonds to neighboring PC headgroups can also be formed. The simulations of the phase diagrams show that all absolute values of ρ_1 become less negative or even positive at pH 4 (see Figs. 6–9).

For low concentrations of the PA component, all four phase diagrams show the same behavior, a considerable broadening of the coexistence range, an almost linear increase in the solidus line, and a more pronounced increase in the liquidus line with increasing acidic component. At high PA content the coexistence range becomes very narrow. The differences in nonideal mixing behavior are much higher at pH 4 than at pH 7. The $\Delta\rho_1$ values are between 650 and 1000 cal/mol. The asymmetry of the mixing behavior seems to be somewhat reduced, but no clear trend is observable for the $\Delta\rho_2$ values (see Figs. 6–9).

An interesting phase behavior is shown by the system DMPA:DPPC. The almost horizontal liquidus line from $x_{DMPA} \approx 0.25-0.75$ indicates that the lipids are not completely miscible in the fluid state and could have an immiscibility gap in this composition range. Historically, the first example of postulated fluid-state lipid immiscibility was the DEPC/DPPE mixture, studied by Wu and McConnell (1975). These results were later contradicted by Silvius (1986). Other examples for fluid-fluid immiscibility have been found recently for two PCs, where one of the PC components has highly asymmetrical chains (Mason, 1988) or mixtures of PC with PS (Hinderliter et al., 1994). This latter case is similar to ours, because the electrostatic repulsion between PS molecules in PC/PS mixtures seems to be overcompensated by other attractive interactions, giving rise to clustering of like molecules. These phase separation processes in pseudobinary systems, i.e., the clustering of lipids, and the formation of microdomains of different composition are phenomena that have raised great interest with respect to their possible biological functions (Lee et al., 1974; Galla and Sackmann, 1975; Jacobson and Papahadjapoulos, 1975; Luna and McConnell, 1977; von Dreele, 1978; Tocanne et al., 1994; Glaser, 1993; Almeida et al., 1993; Vaz, 1994, 1995; Almeida and Vaz, 1995). Fluid domains of different composition could provide membrane proteins with a specific lipid environment necessary for their function.

The DMPA:DPPC mixture is a particularly interesting case in that fluid-fluid immiscibility can be triggered by changing the pH, i.e., the molecular charge of one of the PA components from -1 to approximately -0.7 to -0.5. The phase diagram at pH 4.0 and the calculation of the Gibbs free energy of mixing $\Delta G_{mix} = \Delta G^{ideal} + \Delta G^{E}$, using the nonideality parameters determined from the phase diagram and Eq. 12, clearly suggest a fluid-fluid miscibility gap between $x_{DMPA} = 0.28$ and 0.65, as indicated by the arrows in Fig. 13. Complete miscibility would require that $(\partial^{2}\Delta G_{mix}/\partial x^{2})_{P,\ T} > 0$ over the whole composition range. This is clearly not the case, so that the fluid mixture separates into different phases with compositions indicated by the arrows where the common tangent touches the curve. In contrast to numerous other published diagrams (Huang and Feigenson, 1993), this plot is nonsymmetrical because of our approach of using a two-parameter model for the mixing behavior in each phase.

To illustrate the different mixing behavior at pH 7 and pH 4, we have calculated the lateral distribution of molecules at a mole fraction of $x_{DMPA} = 0.28$ and 0.65 at these two pH values using a Monte Carlo technique (Kawasaki, 1972; Jan et al., 1984), with the nonideality parameters from our simulations of the phase diagram (see Fig. 14). At pH 4 and a mole fraction of $x_{DMPA} = 0.5$, the system separates into two different phases with a lateral distribution of molecules, as shown in the bottom row. Because of the high positive values of the nonideality parameters, like molecules tend to cluster into domains. At $x_{DMPA} = 0.28$, domains of DMPA molecules in a DPPC matrix are formed, whereas at $x_{DMPA} = 0.65$ the reverse effect happens—the DPPC molecules form unconnected domains in a DMPA matrix. At pH 7 the system is mixed and the molecules have a distribution as shown in the top row of Fig. 14. So even outside the composition of the miscibility gap, domain formation can

be induced by a change in pH to lower values, i.e., by partly protonating the PA component.

The form of the phase diagram for DMPA:DPPC at pH 4 suggests that, alternatively, an upper azeotropic point could be present at $x_{DMPA} = 0.6$ instead of a fluid-fluid immiscibility. Our arguments presented above are based on the values of the nonideality parameters obtained from the simulation of the complete phase diagram and the resulting diagram for ΔG_{mix} shown in Fig. 13. The simulation procedure has certain limitations, however. A final decision on whether our suggestions are correct can only be made after additional experiments that are sensitive to fluid-fluid phase separation phenomena.

Effects of sample incubation

We have studied the effect of incubation of samples at 3°C for several days. The reason for this analysis is to know whether the pseudobinary mixtures prepared without incubation are in a thermodynamically stable state and whether sample incubation changes the shape of the thermograms and the form of the phase diagrams.

The samples were prepared as described in Materials and Methods and incubated for 6 days at 3°C. This was done for a representative system, namely DMPA:DPPC at pH 4 and 7. The resulting thermograms are shown in Fig. 4. The dashed lines represent the simulated cp curves as described before.

At both pH values, pure DPPC shows an additional phase transition from the so-called L_{c} subphase to the $L_{\beta'}$ phase (Chen et al., 1980; Lewis et al., 1987). This type of sub-phase transition is also found for phosphatidylglycerols (Wilkinson and McIntosh, 1986). At pH 7.0, we found this phase transition for DPPC at 19.3°C with an enthalpy of 3.6 kcal/mol, in agreement with previous observations. The transition temperature and enthalpy were found to depend on the incubation time at low temperature because the transition to the L_{c} phase is very slow. Therefore, this transition is only observed in first heating scan. At pH 4 the temperature of the subtransition shifts to 18.3°C and the enthalpy of transition decreases to 2.4 kcal/mol. The temperature of the main transition of the preincubated pure lipids (DMPA and DPPC) are compared to the nonincubated pure lipid samples marginally shifted to lower temperatures, and the enthalpies of the main transitions are slightly reduced, but the cooperativity is slightly higher than in nonincubated samples.

Comparing the cp curves of the incubated binary mixtures (Fig. 4) to the nonincubated samples, (Fig. 3) we see that for both pH values and at nearly all mixing ratios, the subtransition has disappeared. The general shapes of the thermograms for the main transitions are nearly identical, although slightly more structured. The second heating scan of these samples has the effect of smoothing the cp curves. No difference is observed for the temperature describing the onset and offset of the coexisting range of the different
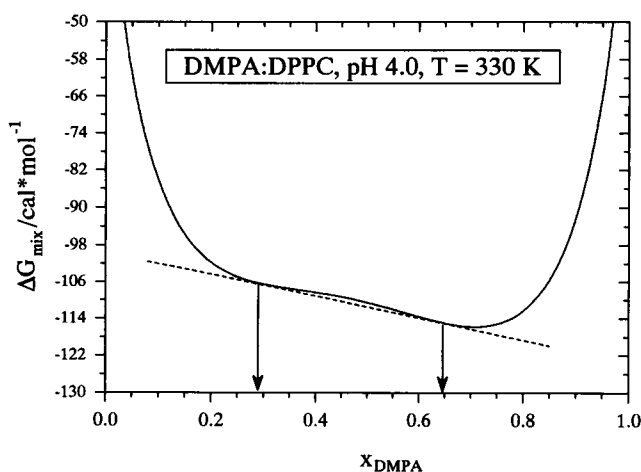

FIGURE 13 Calculation of ΔG_{mix} as a function of x_{DMPA} for DMPA:DPPC mixtures at pH 4.0, using the nonideality parameters shown in Fig. 8. The boundaries of the miscibility gap are indicated by the arrows.

FIGURE 14   Lipid lateral distributions in the liquid-crystalline phase ($T = 330K$) obtained from Monte Carlo simulations for the system DMPA:DPPC at pH 4 and pH 7. For the simulation of the mixture with $x_{DMPA} = 0.28$, the nonideality parameters used were $\varrho_1 = 1354$ cal/mol (pH 4), $\varrho_1 = -151$ cal/mol (pH 7); and for the mixture with $x_{DMPA} = 0.65$: $\varrho_1 = 1313$ cal/mol (pH 4) and $\varrho_1 = 90$ cal/mol (pH 7).
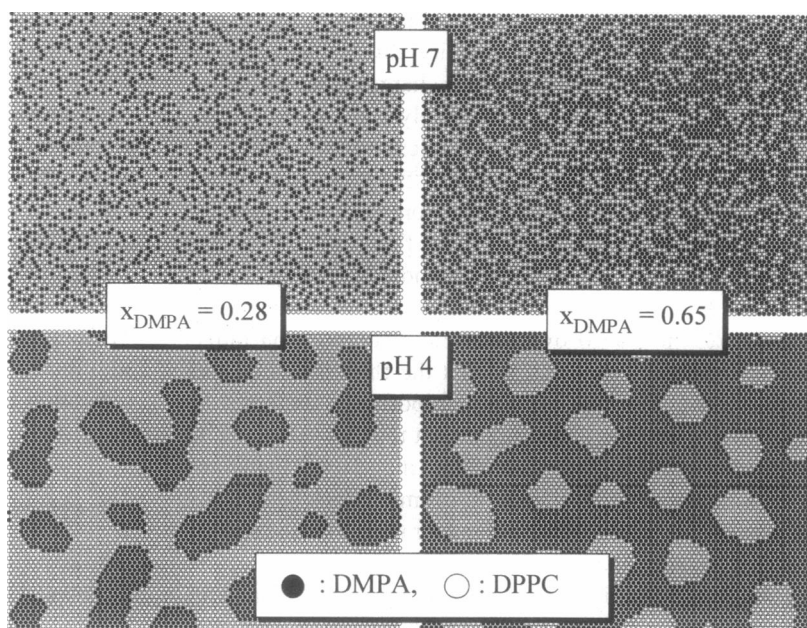
binary mixtures. In Fig. 8 we have shown the T_- and T_+ values obtained from the simulation of the experimental cp curves of the incubated samples as crosses. We see that these temperature values are identical with values obtained from the simulation of the DSC curves of the nonincubated samples. Therefore the $\Delta\varrho$ values also have very similar values. From these results we can deduce that the preparation of our DSC samples has no measurable effects on the properties of the main transition in our mixtures and that data for the coexistence lines can be determined with sufficient precision from experiments with nonincubated samples.

Effects of ionic strength and buffer

The DSC curves of PC-PA mixtures presented here were all obtained with unbuffered samples at low ionic strength, with a total lipid concentration of ~3–4 mM. The pH was adjusted to the required value and checked before and after each experiment and was not found to have changed. It is well known that the apparent pK changes with ionic strength. For a 1 mM DMPA without added salt, the apparent pK for the second dissociation step is ~9, whereas the intrinsic pK is 6.2 at low temperatures and decreases to 5.4 for the liquid-crystalline phase (Eibl and Blume, 1979; Blume and Tuchtenhagen, 1992). For the first dissociation step similar effects are observed, the apparent pK is ~3.8, whereas the intrinsic pK is much lower (~1.5). In our samples at pH 4, the degree of protonation is therefore ~0.3–0.4. When the ionic strength is increased, we would expect similar phase behaviors of the mixtures but at lower pH. This was indeed observed in mixtures of DMPA:DPPC. When the ionic strength was 0.45 M, we had to decrease the pH to 2, to obtain the same phase diagram as observed before at pH 4 for these mixtures under conditions of low

ionic strength (not shown). We have preferred to work under low-ionic-strength conditions to decrease possible acid-catalyzed hydrolysis. This shift is independent of the nature of the added salt, whether it is NaCl or buffer salts.

For measurements at pH 7, the pH is far enough away from the apparent pK_2 that the degree of ionization is essentially constant. For experiments at pH 4, the degree of ionization could change slightly during the transition, because it is possible that the intrinsic pK_1 decreases for liquid-crystalline PA. The medium would then be slightly acidified, counteracting a further increase in dissociation. If buffered suspensions were used, the change in degree of ionization would be larger, because the released protons would be taken up by the buffer and would not lead to a decrease in the pH. As mentioned above, we have decided to use unbuffered media at low ionic strength to reduce the effects of larger changes on degree of ionization and to be able to work at pH 4, where hydrolysis effects are negligible.

Pseudobinary systems at pH 12

As shown in Figs. 1–3 and 5, and in the diagrams for the onset and end of melting in Fig. 12 determined in the usual empirical way, the transitions of the mixtures at pH 12 are very broad. The cp curves as well as the "phase diagrams" could not be successfully simulated by using reasonable values for the nonideality parameters. One would expect that the nonideality parameters become more negative for both phases because of an increase in electrostatic effects, because the PA component is now doubly charged. This would result in a reduction in the width of the two-phase region, as can easily be shown by model calculations (Brumbaugh and Huang, 1992). However, the opposite behavior is observed. The liquidus line is bulging out to higher

temperatures, indicating clustering in the liquid-crystalline phase, i.e., positive nonideality parameters. In addition, the curvatures of the phase boundaries in three of the four mixed systems violate the phase rules. A trial simulation of the phase diagram of DPPA:DMPC mixtures at pH 12, the only phase diagram that is accessible to a simulation (see Fig. 12), gave positive nonideality parameters ρ_1 for both phases in the range of +2.5 kcal/mol and a strong nonsymmetrical mixing behavior. This is highly unlikely and indeed seems to be an artefact caused by the incorrect determination of the temperatures of onset and end of melting.

Experiments at pH 12 must take into account the possibility that during the DSC scan hydrolysis of the lipids will occur and contribute to the enthalpic effects. TLC tests of the samples revealed that after the first scan, hydrolysis (i.e., formation of lysolipids) was below 3% and only became important after the second run, when the sample had been at elevated temperatures for a considerable amount of time. We are therefore relatively sure that the DSC curves shown for the first scan are those for samples with negligible amounts of hydrolysis products. However, at the present time we have no reasonable explanation for the observed thermotropic behavior. A phase separation in the liquid-crystalline phase, i.e., clustering of doubly charged PA molecules as indicated by the positive nonideality parameters, would be very surprising. It would mean that other strongly attractive interactions overcompensate the electrostatic effects.

SUMMARY AND CONCLUSIONS

The phase behavior of PC-PA mixtures was studied at different pH values and therefore at different degrees of ionization of the PA using the DSC method. We employed a newly developed simulation method for a direct determination of the nonideality parameters from the heat capacity curves. These simulations of the cp curves showed that the nonideality parameters were dependent on the PC:PA ratio of the bilayers. Using the temperatures for onset and end of melting determined by the simulations of the cp curves, we then simulated the complete phase diagrams using models for nonideal, nonsymmetrical mixing behavior. The miscibility in PC-PA mixtures strongly depends on pH, i.e., the degree of ionization of the PA component. At pH 7, PA has one negative charge. The nonideality parameters are mainly negative, because of electrostatic repulsion between PA molecules. When the pH is reduced to 4, the PA carries an average charge of −0.6. The reduction in electrostatic repulsion and the increase in attractive interactions between the PA headgroups via hydrogen bonds lead, in some cases, to strongly positive nonideality parameters, which in the case of a DMPA-DPPC mixture results in a fluid-fluid immiscibility, although an upper azeotropic point cannot be excluded. The strongly positive nonideality parameters indicate that clustering of lipid molecules in these binary liquid-crystalline bilayers can be induced by pH changes.

REFERENCES

Ali, S., H.-N. Lin, R. Bitman, and C.-H. Huang. 1989. Binary mixtures of saturated and unsaturated mixed-chain phosphatidylcholines. A differential scanning calorimetry study. Biochemistry. 28:522–528.

Almeida, P. P. F., and W. L. C. Vaz. 1995. Lateral diffusion in membranes. In Structure and Dynamics of Membranes. R. Lipowsky and E. Sackmann, editors. Elsevier Science, Amsterdam. 305–357.

Almeida, P. F. F., W. L. C. Vaz, and T. E. Thompson. 1993. Percolation and fusion in three-component bilayers: effect of cholesterol on an equimolar mixture of two phospatidylcholines. Biophys. J. 64:399–412.

Benga, G., and R. P. Holmes. 1984. Interactions between components in biological membranes and their implications for membrane function. Prog. Biophys. Mol. Biol. 43:195–257.

Berclaz, T., and M. Geoffroy. 1984. Spin-labeling study of phosphatidylcholine-cardiolipin binary mixtures. Biochemistry. 23:4033–4037.

Berclaz, T., and H. McConnell. 1981. Phase equilibria in binary mixtures of dimyristoylphosphatidylcholine and cardiolipin. Biochemistry. 23: 635–640.

Blume, A. 1988. Applications of calorimetry to lipid model membranes. In Physical Properties of Biological Membranes and Their Functional Implications. C. Hidalgo, editor. Plenum Publishing Corporation, New York.

Blume, A. 1991. Biological Calorimetry: Membranes. Thermochim. Acta. 193:299–347.

Blume, A., and H. J. Eibl. 1979. The influence of charge on bilayer membranes. Calorimetric investigations of phosphatidic acid bilayers. Biochim. Biophys. Acta. 558:13–21.

Blume, A., and J. Tuchtenhagen. 1992. Thermodynamics of ion binding to phospholipid bilayers. Titration calorimetry of the heat of dissociation of DMPA. Biochemistry. 31:4636–4642.

Brumbaugh, E. E., and C. Huang. 1992. Parameter estimation in binary mixtures of phospholipids. Methods Enzymol. 210:521–539.

Carruthers, A., and D. L. Melchior. 1983. Studies of the relationship between bilayer water permeability and bilayer physical state. Biochemistry. 22:5797–5807.

Chen, S. C., J. M. Sturtevant, and B. J. Gaffney. 1980. Scanning calorimetric evidence for a third phase transition in phosphatidylcholine. Proc. Natl. Acad. Sci. USA. 77:5060–5063.

Cronan, J. E., and E. P. Gelman. 1975. Physical properties of membrane lipids: biological relevance and regulation. Bacteriol. Rev. 39:232–256.

Eibl, H., and A. Blume. 1979. The influence of charge on phosphatidic acid bilayer membranes. Biochim. Biophys. Acta. 553:476–488.

Galla, H. J., and E. Sackmann. 1975. Chemically induced phase separation in mixed vesicles containing phosphatidic acid. An optical study. J. Am. Chem. Soc. 97:4114–4120.

Garidel, P. 1993. Physikalisch-chemische Untersuchungen zum thermotropen Verhalten von Phospholipiden. Anwendungen der DSD-, DSC-, ²H-NMR- und FT-IR-Methoden. Diploma thesis. University of Kaiserslautern, Kaiserslautern, Germany.

Glaser, M. 1993. Lipid domains in biological membranes. Curr. Opin. Struct. Biol. 3:475–481.

Guggenheim, E. A. 1944. Statistical thermodynamics of mixtures with zero energies of mixing. Proc. R. Soc. Lond. Ser. A. 183:203–212.

Hahn, F. L., and R. Luckhaus. 1956. Ein vorzügliches Reagenz zur kolorimetrischen Bestimmung von Phosphat und Arsenat. Z. Anal. Chem. 149:172–177.

Hildebrandt, H. J. 1929. Solubility (XII). Regular solutions. J. Am. Chem. Soc. 51:66–80.

Hinderliter, A. K., J. Huang, and G. W. Feigenson. 1994. Detection of phase separation in fluid phosphatidylserine/phosphatidylcholine mixtures. Biophys. J. 67:1906–1911.

Hoekstra, D. 1982a. Fluorescence method for measuring the kinetics of Ca^{2+}-induced phase separations in phosphatidylserine-containing lipid vesicles. *Biochemistry.* 21:1055–1061.

Hoekstra, D. 1982b. Role of lipid phase separations and membrane hydration in phospholipid vesicle fusion. *Biochemistry.* 21:2833–2840.

Huang, J., and G. W. Feigenson. 1993. Monte Carlo simulation of lipid mixtures: finding phase separation. *Biophys. J.* 65:1788–1794.

Inoue, T., T. Tasaka, and R. Shimozawa. 1992. Miscibility of binary phospholipid mixtures under hydrated and unhydrated conditions. I. Phosphatidic acids with mixtures of different acyl chain length. *Chem. Phys. Lipids.* 63:203–212.

Jacobson, K., and D. Papahadjopoulos. 1975. Phase transitions and separations in phospholipid membranes induced by changes in temperature, pH, and concentration of bivalent cations. *Biochemistry.* 14:152–161.

Jan, H., T. Lookman, and D. A. Pink. 1984. On computer simulation methods used to study models of two-component lipid bilayers. *Biochemistry.* 23:3227–3231.

Janiak, M. J., D. M. Small, and G. G. Shipley. 1976. Nature of the thermal pretransition of synthetic phospholipids: dimyristoyl- and dipalmitoyl-lecithin. *Biochemistry.* 15:4575–4580.

Janiak, M. J., D. M. Small, and G. G. Shipley. 1979. Temperature and compositional dependence of the structure of hydrated dimyristoyl lecithin. *J. Biol. Chem.* 254:6068–6078.

Johann, C., P. Garidel, L. Mennicke, and A. Blume. 1996. New approaches for the simulation of heat capacity curves and phase diagrams of pseudobinary phospholipid mixtures. *Biophys. J.* 71:3215–3228.

Kawasaki, K. 1972. Kinetics of Ising models. *In* Phase Transitions and Critical Phenomena. C. Domb and M. S. Green, editors. Academic Press, London. 443–501.

Lee, A. G. 1975a. Functional properties of biological membranes: a physical-chemical approach. *Prog. Biophys. Mol. Biol.* 29:3–56.

Lee, A. G. 1975b. Fluorescence studies of chlorophyll a incorporated into lipid mixtures, and the interpretation of "phase" diagrams. *Biochim. Biophys. Acta.* 413:11–23.

Lee, A. G. 1977a. Lipid phase transitions and phase diagrams. I. Lipid phase transitions. *Biochim. Biophys. Acta.* 472:237–281.

Lee, A. G. 1977b. Lipid phase transitions and phase diagrams. II. Mixtures involving lipids. *Biochim. Biophys. Acta.* 472:285–344.

Lee, A. G. 1978. Calculation of phase diagrams for non-ideal mixtures of lipids, and a possible random distribution of lipids in lipid mixtures in the liquid cristalline phase. *Biochim. Biophys. Acta.* 507:433–444.

Lee, A. G., N. J. M. Birdsall, J. C. Metcalfe, P. A. Toon, and G. B. Warren. 1974. Cluster in lipid bilayers and the interpretation of thermal effects in biological membranes. *Biochemistry.* 13:3699–3705.

Lewis, R. N. A. H., N. Mak, and R. N. Mc. Elhaney. 1987. A differential scanning calorimetric study of the thermotropic phase behavior of model membranes composed of phosphatidylcholines containing linear saturated fatty acyl chains. *Biochemistry.* 26:6118–6126.

Luna, E. J., and H. M. McConnell. 1977. Lateral phase separations in binary mixtures of phospholipids having different charges and different crystalline structures. *Biochim. Biophys. Acta.* 470:303–316.

Mabrey, S., and J. M. Sturtevant. 1976. Investigation of phase transition of lipids and lipid mixtures by high sensitivity differential scanning calorimetry. *Proc. Natl. Acad. Sci. USA.* 73:3862–3866.

Mason, J. T. 1988. Mixing behavior of symmetric chain length and mixed chain length phosphatidylcholines in two-component multilamellar bilayers: evidence for gel and liquid-crystalline phase immiscibility. *Biochemistry.* 27:4421–4429.

McIntosh, T. J. 1980. Differences in hydrocarbon chain tilt between hydrated phosphatidylethanolamine and phosphatidylcholine bilayers. *Biophys. J.* 29:237–246.

McLaughlin, S., and J. Brown. 1981. Diffusion of calcium ions in retinal rods. A theoretical calculation. *J. Gen. Physiol.* 77:475–487.

Mennicke, L. 1995. Die Simulation der Wärmekapazitätskurven und die Berechnung der Phasendiagramme von pseudobinären Lipid-Lipid-Wasser Systemen am Beispiel von gemischtkettigen Phospholipiden mit verzweigten Acylketten. Ph.D. thesis. University of Kaiserslautern, Kaiserslautern, Germany.

Metcalf, T. N., J. L. Wang, and M. Schindler. 1986. Lateral diffusion of phospholipids in the plasma membrane of soyabean protoplasts: evi-

dence for membrane lipid domains. *Proc. Natl. Acad. Sci. USA.* 83:95–99.

Nibu, Y., T. Inoue, and I. Motoda. 1995. Effect of headgroup type on the miscibility of homologous phospholipids with different acyl chain lengths in hydrated bilayer. *Biophys. Chem.* 56:273–280.

Shimshick, E. J., and H. M. McConnell. 1973. Lateral phase separation in phospholipid membranes. *Biochemistry.* 12:2351–2360.

Silvius, J. R. 1986. Solid- and liquid-phase equilibria in phosphatidylcholine/phosphatidylethanolamine mixtures. A calorimetric study. *Biochim. Biophys. Acta.* 857:217–228.

Silvius, J. R., and J. Gagné. 1984a. Lipid phase behavior and calcium induced fusion of phosphatidylethanolamine-phosphatidylserine vesicles. Calorimetric and fusion studies. *Biochemistry.* 23:3232–4340.

Silvius, J. R., and J. Gagné. 1984b. Calcium-induced fusion and lateral phase separation in phosphatidylcholine-phosphatidylserine vesicles. Correlation by calorimetric and fusion measurements. *Biochemistry.* 23:3241–4347.

Stier, A., and E. Sackmann. 1973. Spin labels as enzyme substrates. Heterogeneous lipid distribution in liver microsomal membranes. *Biochim. Biophys. Acta.* 311:400–408.

Sugár, I. P. 1987. Cooperativity and classification of phase transitions. Application to one- and two-component phospholipid membranes. *J. Phys. Chem.* 91:95–101.

Tardieu, A., V. Luzzati, and F. C. Reman. 1973. Structure and polymorphism of the hydrocarbon chains of lipids: a study of lecithin-water phases. *J. Mol. Biol.* 75:711–733.

Tenchov, B. 1985. Nonuniform lipid distribution in membranes. *Prog. Surf. Sci.* 20:273–340.

Tocanne, J.-F., L. Cézanne, A. Lopez, B. Piknova, V. Schram, J.-F. Tournier, and M. Welby. 1994. Lipid domains and lipid/protein interactions in biological membranes. *Chem. Phys. Lipids.* 73:139–158.

Tokutomi, S., K. Ohki, and S.-I. Ohnishi. 1980. Proton-induced phase separation in phosphatidylserine/phosphatidylcholine membranes. *Biochim. Biophys. Acta.* 596:192–200.

Träuble, H. 1976. Membrane electrostatics. *In* Structure of Biological Membranes. S. Abrahamsson and I. Pascher, editors. Plenum Press, New York. 509–550.

Träuble, H., and H. J. Eibl. 1974. Electrostatic effects on lipid phase transitions: membrane structure and ionic environment. *Proc. Natl. Acad. Sci. USA.* 71:214–219.

Träuble, H., M. Teubner, P. Woolley, and H. Eibl. 1976. Electrostatic interactions at charged lipid membranes. 1. Effects of pH and univalent cations on membrane structure. *Biophys. Chem.* 4:319–342.

Tuchtenhagen, J. 1994. Kalorimetrische und FT-IR-spektroskopische Untersuchungen an Phospholipidmodellmembranen. Ph.D. thesis. University of Kaiserslautern, Kaiserslautern, Germany.

van Dijck, P. W. M., A. J. Kaper, H. A. J. Oonk, and J. De Gier. 1977. Miscibility properties of binary phosphatidylcholine mixtures. A calorimetric study. *Biochim. Biophys. Acta.* 470:58–69.

Vaz, W. L. C. 1994. Diffusion and reaction in phase-separated membranes. *Biophys. Chem.* 50:139–145.

Verkleij, A. J. 1984. Lipid intramembrane particles. *Biochim. Biophys. Acta.* 779:43–63.

Verkleij, A. J., B. De Kruyff, P. H. Ververgaert, J. F. Tocanne, and L. L. M. van Deenen. 1974. The influence of pH, Ca^{2+}, and protein on the thermotropic behaviour of the negatively charged phospholipid, phosphatidylglycerol. *Biochim. Biophys. Acta.* 39:432–437.

Vaz, W. L. C. 1995. Percolation properties of two-component, two-phase phospholipid bilayers. *Mol. Membr. Biol.* 12:39–43.

von Dreele, P H. 1978. Estimation of lateral species separation from phase transitions in non-ideal two-dimensional lipid mixtures. *Biochemistry.* 17:3939–3943.

Wilkinson, D. A., and T. J. McIntosh. 1986. A subtransition in a phospholipid with a net charge, dipalmitoylphosphatidylglycerol. *Biochemistry.* 25:295–298.

Wu, S. H., and H. M. McConnell. 1975. Phase separation in phospholipid membranes. *Biochemistry.* 14:847–854.

Xu, H., F. A. Stephenson, and C.-H. Huang. 1987. Binary mixtures of asymmetric phosphatidylcholines with one acyl chain twice as long as the other. *Biochemistry.* 26:5448–5453.